Uncouple Nonlinear Modeling of Seismic Soil-Pile-Superstructure Interaction in Soft Clay

S. N. Moghaddas Tafreshi

Received: January 2008; Accepted: June 2008

Abstract: *This paper presents the numerical analysis of seismic soil-pile-superstructure interaction in soft clay using free-field soil analysis and beam on Winkler foundation approach. This model is developed to compute the nonlinear response of single piles under seismic loads, based on one-dimensional finite element formulation. The parameters of the proposed model are calibrated by fitting the experimental data of large-scale seismic soil-pile-structure tests which were conducted on shaking table in UC Berkeley. A comparative evaluation of single piles shows that the results obtained from the proposed procedure are in good agreement with the experimental results.*

Keywords: *Seismic analysis; Soil-pile-superstructure interaction; Winkler side-soil springs; Free field analysis.*

1. Introduction

The coincidence of major pile-supported structures sited on soft soils in areas of earthquake hazard results in significant demands on these deep foundations. Possible resonance effects between longer period soft soil sites, which may amplify ground motions and large structures, can exacerbate the problem. Historically, it has been common practice in seismic design to ignore or simplify the influence of pile foundations on the ground motions applied to the structure. This is generally accepted as a conservative assumption in design for a spectral analysis approach, as the flexible pile foundation results in period lengthening, increased damping, and consequently decreased structural forces related to a fixed base case. It is common to evaluate pile integrity during seismic loading, though it is also accomplished with simplified and non-standardized analysis methods. However, in observations of pile performance during earthquakes, two principal facts emerge: firstly pile foundations do affect the ground motions that the superstructure experiences and secondly the piles can suffer extreme damage and failure under earthquake loading.

Various approaches have been used for the dynamic response analysis of pile-supported structures. In analysis, they are usually characterized by the different ways of treating the soil medium. A 2-D or 3-D finite element analysis is definitely a powerful method, but modeling a soil–pile system and setting numerical parameters for the entire model is indeed laborious and the computational effort can be very time consuming [1–3]. Moreover, direct methods require both soils and structures to be treated with equal rigor and complex variations of soil profile in a 2-D or 3-D space should be provided for the analysis. Hence, there still remains an important place for simple approaches even in these days that highly complex numerical solutions are available for difficult problems. It has been customary in engineering practice to assume that a pile is supported by distinct side-soil springs (Winkler hypothesis) [4–9].

In this paper, a rational seismic design method for soil-pile-superstructure interaction is established based on large shaking table on pile-structure model [10]. Initially, the free field motions are calculated separately through a site response analysis using DYFRA program (developed by the author). Secondly, the motions in the form of displacement time history are used as input boundary conditions for a beam (pile) on nonlinear Winkler model to evaluate the response of the pile. This model is composed of a linear elastic beam-column representing the pile, non-linear p-y springs and linear dashpots representing the surrounding soil. The results are also compared with those of the physical model to confirm that our simulations can predict the behavior of pile with acceptable accuracy.

Associate Professor, Department of civil engineering, K .N. Toosi University of Technology E-mail: nas_moghaddas@kntu.ac.ir

2. Description of Shaking Table Test

As mentioned before, the study presented here focuses on simulation of the seismic behavior of soil-pile superstructure interaction which is performed based on a large shaking table [10]. In this experimental program, a series of scaled physical model tests have been performed at U.C. Berkeley on the shaking table to examine the seismic response of soil-pile-structure interaction.

The shaking table is 6.1 m x 6.1 m, with a payload capacity of 580 kN, a bandwidth of 0 - 20 Hz and has recently been upgraded to have six controlled degrees of freedom. The model container confines a soil column, 2.3 m in diameter and up to 2.0 m in height, mounted on the shaking table.

A model soil with appropriately scaled stiffness and strength properties was developed for the experiments, consisting of 72% Kaolinite, 24%Bentonite, and 4% type C fly ash (by weight). The model soil has a unit weight of 14.8 KN/m^3, a plasticity index of 75% and undrained shear strength of 4.8 kPa. The shear strength profile corresponded to a lightly over-consolidated soft to medium stiff clay (layers 1-8), overlying a hard clay bearing layer (layer 9). The soil characteristics and parameters used in the analysis are represented in Table 1.

The flexural rigidity of the prototype pile was computed as 79.120 kN.m^2. Accordingly, the model piles were fabricated using 51mm diameter 6061 T-6 aluminum tubing with a wall thickness of 0.71 mm, which provided the correctly scaled flexural rigidity (EI). The fixity conditions of the pile are known to be significant in lateral response, so the piles are fixed against rotation at the head, and fixed against transition at the tip. This corresponds to a pile driven into a firm stratum at the base and cast into the pile cap. The piles height is approximately 2m and the masses in the head of pile are ranging from 4.5 to 72.7kg.

The layout of tests is shown in Fig. 1. It consisted of four single piles (S1, S2, S3 and S4) with head the masses. The vertical arrays of accelerometers were located within 0.5 m of the piles, but were out of the line of shaking.

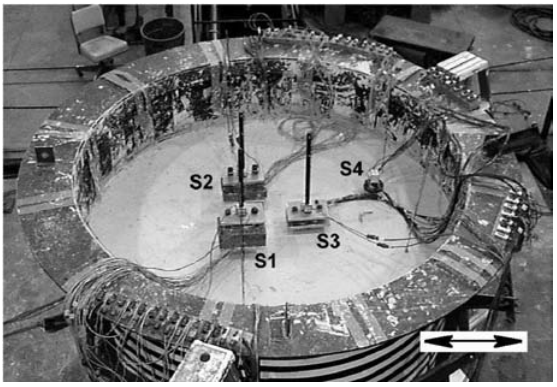

Fig. 1 Configuration of Shaking Table Test [10].

Table 1 Soil properties of layers [10]

Layer Number	Soil Material Type	Thickness of Layers (m)	Maximum Shear Modulus (Mpa)	Total Unit Weight (kN/m^3)	Shear Wave Velocity (m/sec.)	Location of Input Motion	Vertical Effective Stress (kpa)
1	1 (soft to medium)	0.2	0.49	14.80	18.09		0.51
2	1	0.3	0.82	14.80	23.25		1.62
3	1	0.3	1.22	14.80	28.43		3.04
4	1	0.5	1.55	14.80	32.04		4.94
5	1	0.5	1.97	14.80	36.18		7.33
6	1	0.5	3.64	14.80	49.10		9.72
7	1	0.3	5.06	14.80	57.89		11.61
8	1	0.2	9.48	14.80	79.25		12.74
9	2 (bearing layer)	0.2	46.09	18.00	158.49		13.74
			89.70	22.00	200.00	OUTCROP	14.37

The model was subjected to a series of seismic events including sine sweeps and earthquake records. A scaled version (a_{max}=0.20g) of the motion recorded at Yerba Buena Island during the Loma Prieta earthquake was used as the shaking table command signal for the test analyzed herein (Fig. 2).

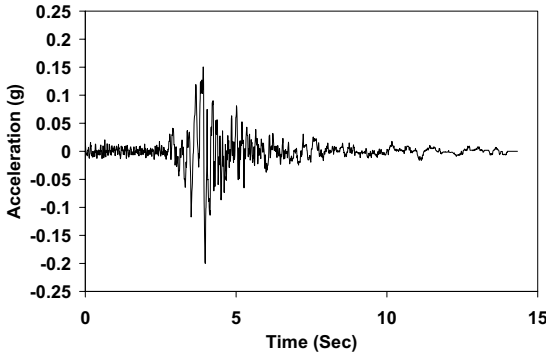

Fig. 2 Scaled acceleration of the motion recorded at Yerba Buena Island during the Loma Prieta earthquake [10].

3. Simulation of the Shaking Table Test Experiments

The governing equation for the soil–pile (equivalent upright beam) interaction model has been driven assuming that the piles were embedded upright in a linear or non linear soil stratum with an infinite lateral extent spreading over rigid horizontal bedrock. Thus, a complex stiffness matrix $[K_{soil}]$ in the frequency domain describes the side-soil impedance for the pile and therefore, when the pile in Fig. 3 is subjected to a lateral displacement along its depth, the equation of equilibrium for soil–pile system is written as:

$$\{F_{ext}\}+[K_{pile}]\{u_{pile}\}+[K_{soil}]\{\{u_{pile}\}-\{u_{free}\}\}=0 \qquad (1)$$

Where vector $\{F_{ext}\}$ denotes the external load on the pile cap from the superstructure, $[K_{pile}]$ and $\{u_{pile}\}$ are pile stiffness matrix and its lateral deformation vector respectively and $\{u_{free}\}$ is the free field ground motion. From Eq. (1), lateral soil reaction forces on the pile group are written in the following form as:

$$\{P_{pile}\}=|[K_{soil}]\{\{u_{pile}\}-\{u_{free}\}\}| \qquad (2)$$

Extracting diagonal terms k_i (i= 1, 2,…, n) of the side-soil stiffness matrix $[K_{soil}]$, Eq. (2) is rewritten as:

$$\{P_{pile}\}=\{k_1u_{pile,1}\quad k_2u_{pile,2}.....k_nu_{pile,n}\}^T-\{P_{off-diag}\} \qquad (3)$$

With

$\{P_{off-diag}\}=$ off- diagonal terms of $[K_{soil}]\{u_{pile}\}-[K_{soil}]\{u_{free}\}$ (4)

Eqs. (1)– (4) yield the expression as follows:

$$\{P_{pile}\}=\begin{bmatrix} k_1 & 0 & .....0 \\ 0 & k_2 & .....0 \\ ..... & & \\ ..... & & \\ 0 & 0 & .....k_n \end{bmatrix}\{\{u_{pile}\}-\{u_{far}\}\} \qquad (5)$$

With

$$\{u_{far}\}=\left\{\frac{\{P_{off-diag}\}}{k_i}\right\} \qquad (6)$$

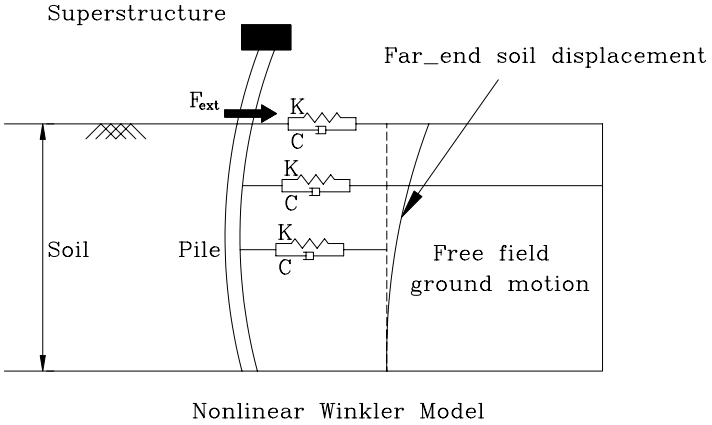

Fig. 3 Schematic of dynamic nonlinear p–y element for soil–pile–structure interaction.

Eq. (5) indicates that a Winkler model can describe the soil–pile interaction. Differing from the conventional Winkler model, Eq. (5) shows the necessity of subtracting a displacement vector $\{u_{far}\}$ from $\{u_{pile}\}$. The vector$\{u_{far}\}$ is interpreted as a displacement given on the other end of the Winkler side-soil springs, and therefore, will be referred to as 'far-end displacements' (Fig. 3). In the following discussion, the free field ground motion $\{u_{free}\}$ $\{u_{free}\}$ included in the far-end displacements $\{u_{far}\}$ will be separated since they will be given as known input values for kinematic interaction effects. The following far-end displacements $\{u_{far}\}$are therefore only due to the inertia interaction.

Excluding$\{u_{free}\}$, the side-soil stiffness matrix in Eq. (2) together with $\{u_{pile}\}$ determines the far-end displacements $\{u_{far}\}$. In other words, the far-end displacements will be strongly affected by the deformation of the pile.

For the uncoupled analysis, the solution precedes two steps, namely, the computation of free field motions and the analysis of the pile-structure response. The "free field" describes the site response in the absence of the structure. The free field motions are calculated separately through a site response analysis and the motions in the form of displacement or acceleration time history are then used in the second stage as input boundary conditions in nonlinear Winkler model.

3.1. Free-Field Soil Analysis

At a large distance from pile foundation (the so called free-field), the motions of these piles have a smaller effect on soils and the one-dimensional wave propagations are adequately assumed for the behavior of layered soil deposits. Because of using the results of shaking table tests, the free-field response of the container was evaluated by comparing the motions recorded at two of the vertical arrays placed inside the container with those of the numerically simulated. As a result, the equivalent linear method of analysis in the frequency domain was used for describing the site response.

A computer program was written for the free field procedure formulations in frequency domain dependent approach in DYFRA program which can be used to solve the ground response problem. In simple terms, the input motion is represented as the sum of a series of sine waves. A relatively simple solution for the response of the soil profile to sine waves of different frequencies (in term of transfer function) is used to obtain the response of the soil deposit to each of the input sine waves. The overall response is obtained by summing the individual response to each of the input sine waves.

The shear modulus and the damping factor of the soil layers are the two main parameters which should be determined by calibration. The calibration is carried out by DYFRA program. In the first step the value of shear modulus and damping factor are selected to correspond with the small value of shear strain (=0.001%). In the next steps the value of maximum shear strain, effective shear strain and its shear modulus and damping factor are obtained. This procedure continues until the difference of the two obtained values in two consecutive steps becomes negligible. On the other hand, convergence in calculating should be provided. Consequently, the final obtained value of shear modulus and damping factor apply to free-field soil analysis.

Fig. 4 shows the comparison of the recorded spectral acceleration from the experimental data of large-scale seismic soil-pile-structure tests and the result of free-field analysis (obtained of DYFRA program) for second, fourth, sixth and eighth layers. The comparison between the results of the analysis and the experiment show good consistency and satisfactory accuracy. For all of the layers, the best coincidence of spectral acceleration is obtained for high periods. Overall, the analysis can predict the values of spectral acceleration for magnitudes of period greater than 0.2 second with good accuracy. In other words, the maximum difference takes place for high frequencies (f >5Hz.). The peak acceleration happened in a period less than T=1 sec. This fact confirms the presented typical spectral acceleration by API code and also notability of local site effect in soft clay.

Fig. 5 shows the recorded displacement for second, fourth, sixth and eighth layers obtained of DYFRA program. The results state that the magnitude of displacement (and maximum displacement) reduces from second layer to eighth layer, significantly. Also the maximum displacement for all the layers happened in time of 4.2 sec.

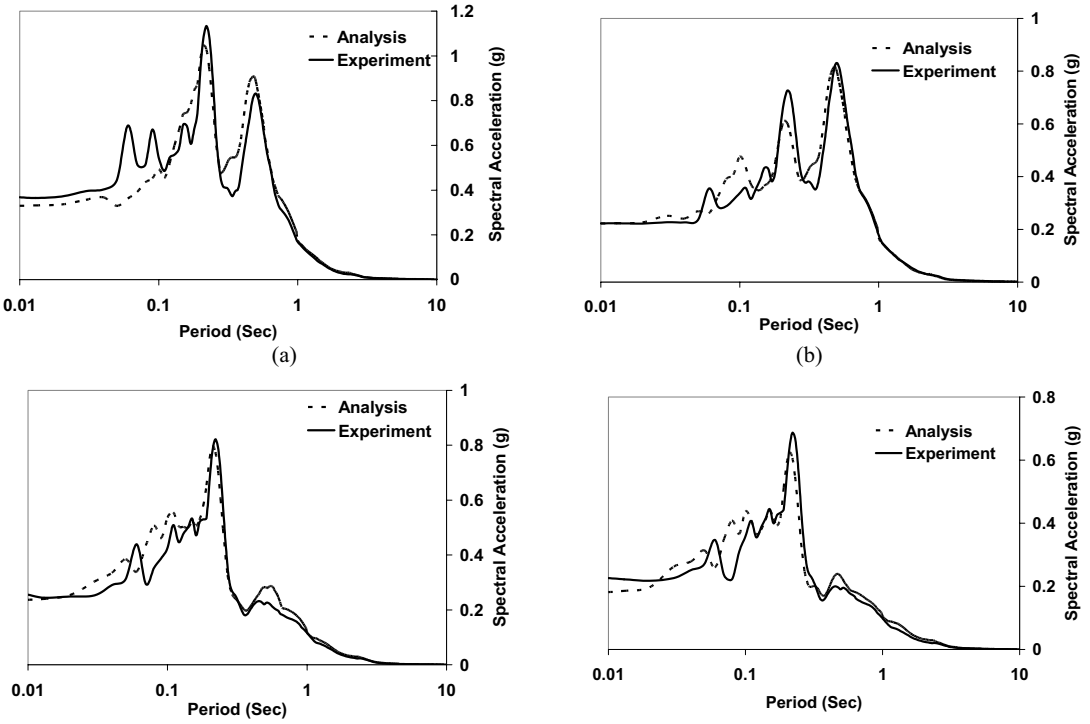

Fig. 4 Comparison of the recorded spectral acceleration from the test and DYFRA program (a) second layer; (b) fourth layer; (c) sixth layer; and (d) eighth layer.

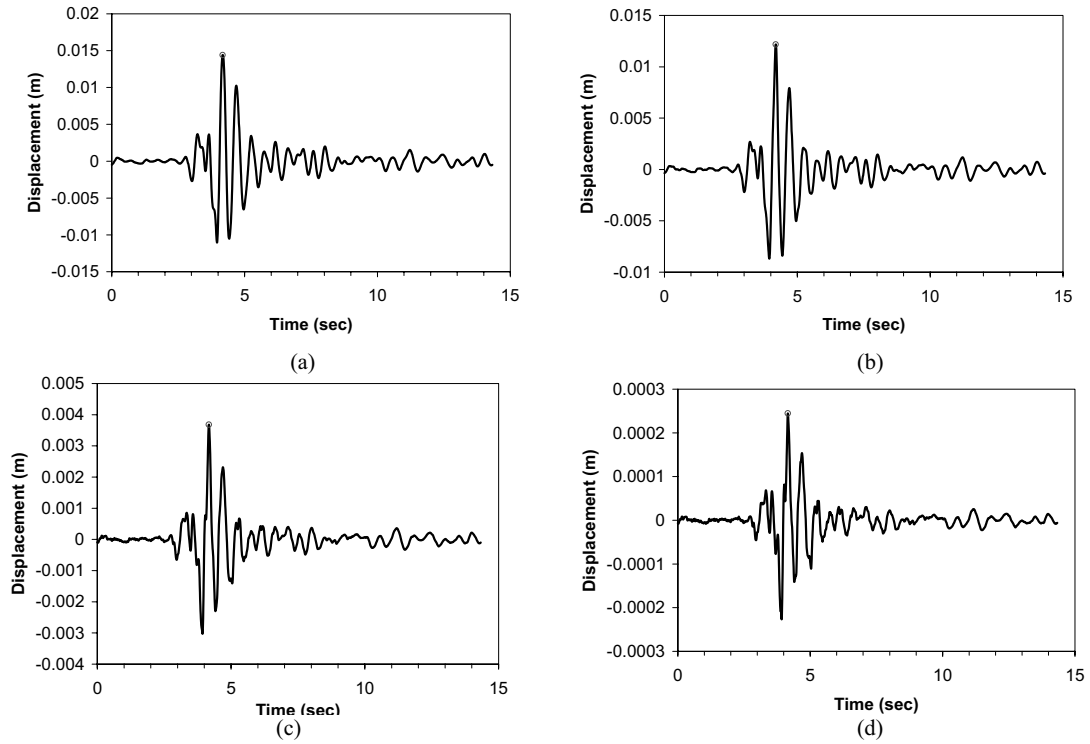

Fig. 5 Recorded displacement from DYFRA program (a) second layer; (b) fourth layer; (c) sixth layer; and (d) eighth layer.

3.2. Winkler side-soil springs

As described before, the problem herein is that of a single pile embedded in layered soft clay and subjected to lateral motion induced by a shaking table. The surrounding soil is considered to be a homogeneous deposit with shear wave velocity V_s, density ρ_s, shears strength $S = S_u(z)$, which varies with depth. The soil–pile interface is modeled as a Winkler foundation interacting with the pile through nonlinear springs at near surface and with linear springs at deep depth; along with these elements linear dashpots are used. Fig. 6 shows the model of pile-superstructure, non-linear p-y springs and linear dashpots representing the surrounding soil layers. The outputs of the free field analysis for each layer in the form of displacement time history are applied as input boundary conditions in the free end of the nonlinear Winkler side-soil springs in ANSYS 5.4 program [11]. The length of the pile is divided to 9 segments (8 segments embedded in the soil and one segment is out of the soil surface). The masses in the head of the piles S1, S2, S3, and S4 to model the effect of superstructure are respectively, 4.5, 11.25, 45, 72.7 kg. The schematic layout model of the piles and superstructure and the uncoupled seismic soil-pile-superstructure diagram are shown in Fig. 6. The Winkler model requires a definition of parameters for the nonlinear springs as well as the viscous dashpots.

Based on a number of analytical studies that compare the pile head displacements from the Winkler model analyses with 3-D finite element analyses, the stiffness of the soil springs per unit length under lateral loading can be approximated realistically by Eq. (7) [12, 13]:

$$k_x \approx 1.2E_s(z) \tag{7}$$

Where k_x is the stiffness of the continuously distributed spring and $E_s(z)$ is the Young's modulus of the soil as a function of depth z. The value in Eq. (7) is multiplied by the spacing between the two adjacent springs to obtain the discrete spring stiffness.

The stiffness of spring k which has a linear behavior at high depth is recommended by Eq. (8) [12, 13]:

$$k = \frac{8\pi G_m(1-\nu)(3-4\nu)\left[(r_0/r_1)^2+1\right]}{(r_0/r_1)^2+(3-4\nu)^2\left[(r_0/r_1)^2+1\right]\ln(r_1/r_0)-1} \tag{8}$$

Where r_0 and r_1 are the inner and outer radii of the inner field around the pile, respectively, ν is the Poisson's ratio of the soil and G_m is modified shear modulus calculated according to the strain level. The maximum force in the nonlinear spring at depth z is equal to the ultimate lateral reaction per unit length of the pile at depth z. For cohesive soils, the lateral soil strength based on the theoretical studies [4, 13] using the theory of plasticity under plane-strain conditions is given by Eq. (9):

$$F_{S,\max}(z) = \lambda(z)S_u(z)d\xi \tag{9}$$

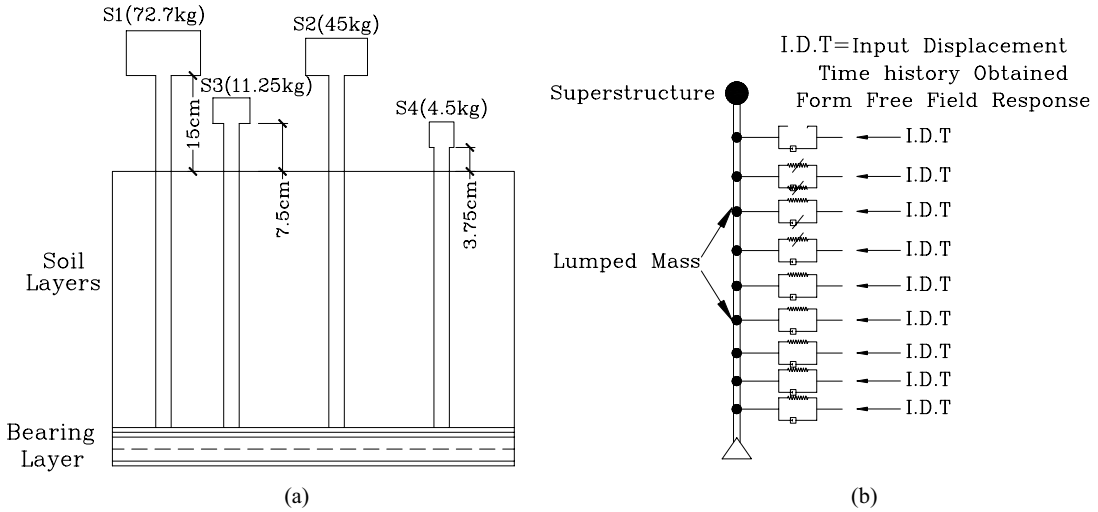

Fig. 6 (a) Schematic model of piles and superstructure; (b) Uncoupled seismic soil- pile-superstructure diagram.

Where d is the pile diameter, $S_u(z)$ is the variation of shear strength with depth and λ is a dimensionless parameter that varies linearly from 3 to 9 [4]. Nevertheless, the following expression for the variation of λ with depth is recommended by Eq. (10) [4]:

$$\lambda(z) = 3 + \frac{\sigma_z}{S_u(z)} + J\frac{z}{d} \tag{10}$$

Here, σ_z is the overburden pressure, and ξ is a hysteretic dimensionless quantity that is governed by the following nonlinear equation:

$$y_\circ \dot{\xi} + \gamma|\dot{y}|\xi|\xi|^{n-1} + \beta\dot{y}|\xi|^n - A\dot{y} = 0 \tag{11}$$

In which y is the pile deflection at the location of the spring, and y_0 is the yield limit defined by $y_0 = S_u(z)/k$, where k is the small-amplitude distributed elastic stiffness usually approximated by [10, 12]. Also, β, γ, n and A (=1 in this paper) are dimensionless quantities that control the shape of the hysteretic loop. The coefficients J and n are the two main coefficients that should be obtained by calibrating the model for near field against known experimental data. Hence, the maximum force (or strength) of the spring is obtained by multiplying the maximum reaction force of the soil in Eq. (10) with the spacing between the two adjacent springs, s.

At small-amplitude linear limits, the restoring force from the dashpot is in the form of Eq. (12) which is recommended by [14-15].

$$c(a_0, z) = \left[Qa_0^{-0.25}\rho_s V_s d\right] s \tag{12}$$

Where c is the dashpot coefficient and the term within the brackets is the distributed frequency dependent damping coefficient. Also a_0 is a dimensionless frequency parameter ($=\omega d/V_s$), ω is the angular frequency, ρ_s is the soil density, V_s is the shear wave velocity in the soil medium, d is the pile diameter, and s is the spacing between the two adjacent dashpots. The coefficient Q is given by the expression:

$$Q = \begin{cases} 3 & if \quad z<3d. \\ 2\left[1+\dfrac{3.4}{\pi(1-\nu)}\right]^{1.25}\left(\dfrac{\pi}{4}\right)^{0.75} & if \quad z>3d. \end{cases} \tag{13}$$

Where ν is the Poisson's ratio of the soil.

With the above formulation, the nonlinear spring equation and the dashpot equation of the constitutive model are consistent with the viscoplastic analysis at the limit of small deflections and the plasticity analysis at the zero-frequency limit.

The coefficients J, n and also the near field parameters (shear wave velocity; V_s and Poisson's ratio; ν) should be determined by calibrating the model against results of the shaking table experimental data for the piles S1, S2, S3, and S4. Table 2 shows the values of these parameters which are obtained by calibration.

Then the values of calibrated parameters in Table 2 are introduced to ANSYS 5.4 [11] program as model parameters to investigate the behavior of the piles. The output results of the analysis are included in the form of a time history of displacement and acceleration of superstructure, and also acceleration of lumped mass at the nodes of pile.

Fig. 7 compares the experimental data with the computed acceleration of superstructure for the piles S1, S2, S3, and S4. The observed values show that, the maximum acceleration occurs in the pile S1, S2, S3 and S4, respectively. The reason is that the concentrative mass on the head of the piles and the free length of the piles above the level of soil increases from the pile S4 to S1 (see Fig. 6-a).

The computed results are in a reasonable agreement with the experimental values, indicating that the proposed p–y model is promising in estimating acceleration of superstructure, distributions of the bending moment and displacement of piles and thus may be convenient to be used as a tool for designing pile foundations in engineering design of piles. It should be noted that the effect of pile group and influence of wave reflection for used analytical models are not considered in this procedure and it may be account for the difference between the results of the analysis and those of the experiments.

Table 2 The values of calibrated parameters.

Pile Number	J	n	V_s (m/sec.)	ν
S1	0.0047	0.25	23.25	0.4
S2	0.0027	0.55	28.43	0.4
S3	0.0021	0.85	32.04	0.4
S4	0.0019	1	36.18	0.4

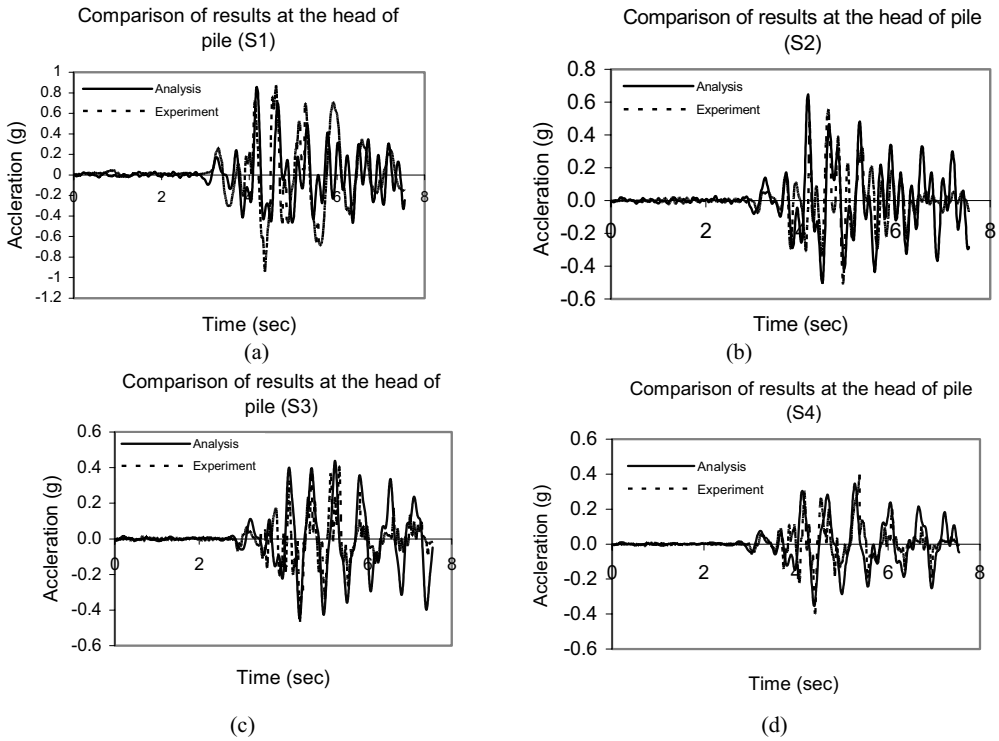

Fig. 7 Comparison of the recorded acceleration of superstructure from the test and Winkler side-soil springs model (a) pile S1; (b) pile S2; (c) pile S3; and (d) pile S4.

4. Conclusions

The uncoupled nonlinear Beam-on-Winkler foundation model and site response analysis used in the method proposed in this research provide a convenient method for an extensive study of soil-pile-structure interactions. The responses of free-field and single piles analysis were calculated and compared with the results observed in the large shaking table. Based on the analyses performed in this study, the following general conclusions made:

1. The estimated spectral accelerations of the free-field analysis for various soil layers are in good agreement with those obtained from the experiments. The peak acceleration for all layers of soil happened in a period less than 1 second; this fact confirms the notability of local site effect in soft clay. Overall, these results suggest that the result of DYFRA program is promising for estimating the spectral acceleration of soil layers with a reasonable degree of accuracy.
2. Comparisons between the obtained acceleration for the superstructure of the Beam-on-Winkler foundation model and those of the experiments reveal that there is a good agreement between the two approaches. These agreements clarify that the proposed method is a reliable method for predicting the soil-pile-superstructure behavior subjected to seismic loading.

Although the results obtained in the present paper are encouraging for considering the uncoupled Beam-on-Winkler foundation model in investigating the soil-pile-structure interaction, but it should be noted that the numerical results are obtained for only one type of soil (soft clay). Hence the values of calibrated parameters in Table 2 are limited to soil characteristics and the tests conditions used. In other words, the obtained calibrated parameters can be applied to soft clay soil in this study and other studies with similar grading, plasticity index and characteristics. Also the proposed uncoupled model is compared to only one case study. Therefore the verification of this model with other experimental works, in field or full-scale tests on various conditions such as different soils, various heights of pile and masses in the head of the pile can prove very useful. But this subject is out of the scope limits of the current paper;

however it could be a topic worth considering for further research.

References

[1] Kimura M, Zhang F. Seismic evaluations of pile foundations with three different methods based on three- dimensional elasto-plastic finite element analysis. Soils Found 2000; 40(5):113–32.

[2] Wakai A, Gose S, Ugai K. 3-D elasto-plastic finite element analyses of pile foundations subjected to lateral loading. Soils Found 1999; 39(1):97–111.

[3] Yang Z, Jeremic B. Numerical study of group effects for pile groups in sands. Int J Numer Anal Methods Geomech 2003; 27:1255–76.

[4] Matlock H. Correlations of design of laterally loaded piles in soft clay. In: Proceedings of the offshore technology conference, vol. 1(1204) Houston, TX, 1970. p. 577–94.

[5] Reese L. C., Cox W. R., Koop F. D. Analysis of laterally loaded piles in sand. In: Proceedings of the sixth offshore technology conference, paper 2080, Houston, TX, 1974. p. 473–83.

[6] Zhang L. M. M., Lai P. Numerical analysis of laterally loaded 3 _ 3 to 7 _ 3 pile groups in sands. J Geotech Geoenviron Engin 1999; 125(11): 936–46.

[7] Wang S, Kutter B. L., Chacko J. M., Wilson D. W., Boulanger R. W., Abghari A. Nonlinear seismic soil–pile–structure interaction. Earthquake Spectra 1998; 14(2): 377–96.

[8] Boulanger R. W., Curras C. J., Kutter B.L., Wilson D. W., Abghari A. Seismic soil–pile–structure interaction experiments and analyses. J Geotech Geoenviron Eng ASCE 1999; 125(9):750–9.

[9] Tahghighi H, Konagai K Numerical analysis of nonlinear soil–pile group interaction under lateral loads. Soil Dyn. Earthquake Eng 2007; 27: 463–474

[10] Maymand, P., Reimer, M. and Seed R. Large Scale Shaking Tables Tests of Seismic Soil-Pile Interaction in Soft Clay. Proc.12th World Conf.Earthquake Eng. New Zealand, 2000; Vol.5, No.0915.

[11] Kohnke, P. ANSYS Theory Reference Release 5.4: 8th Edition., 1997; ANSYS, Inc.

[12] Gazetas, G. and Dobry, R., Horizontal Response of Piles in Layered Soils, J. Geo. Eng., ASCE, 1984; 110(1), 20-40.

[13] Makris, N. and Gazetas, G.,. Dynamic Pile-Soil-Pile Interaction – Part II: Lateral and Seismic Response, Earthquake Eng.Struct.Dyn, 1992; 21(2), 145-162.

[14] Badoni, D. and Makris, 1996, N., Nonlinear response of single piles under lateral inertial and seismic loads. Soil Dyn Earthquake Eng 1996; 43: 15-29

[15] Badoni, D. and Makris, N.,. Analysis of Nonlinear Response of Structures Supported on Pile Foundations. Rpt. No. UCB/EERC-97/07, 1997; Earthquake Eng. Research Ctr., Univ. of California.